An Impulse Radio Asynchronous Transceiver for High Data Rates

Stéphane Paquelet[1], Louis-Marie Aubert[1] and Bernard Uguen[2]
(1) Mitsubishi ITE-TCL, Rennes, France, (2) IETR-INSA, Rennes, France
Email: paquelet@tcl.ite.mee.com

***Abstract*— The purpose of this paper is to provide an operative way of achieving high data rates for Impulse Radio (IR) transmission based systems. Since applications targeted for Ultra Wide Band (UWB) are liable to be low-cost, we especially focus on simple transceiver design. To that effect, we present an original demodulation scheme adapted to a multi-band On-Off Keying modulation.**

From the receiver point of view, we impose relaxed channel estimation constraints and derive suitable signal processing schemes and simple hardware architectures. Indeed, we only consider the benefit from a limited *a priori* channel knowledge: approximative delay spread and energy level. The associated optimum demodulation turns out to be a non-trivial energetic threshold comparison whose precise theoretical computation admits an analytical solution proving its feasibility.

Numerical results are eventually performed for IEEE 802.15.3a channel models and FCC requirements; they obviously demonstrate the potential of these techniques.

***Index Terms*— Impulse Radio, UWB, High data rates, Non-coherent OOK, chi-square law.**

I. INTRODUCTION

Considering *Ultra Wide Band* (UWB) radio link, in accordance with the American *Federal Communications Commission* (FCC) regulation, we aim at designing a simple transmitter/receiver architecture suitable for High Data Rates. *Wireless Personal Area Network* (WPAN) issues are especially targeted taking into account IEEE 802.15.3a requirements.

From a general point of view, research in UWB started several decades ago, and the first patent applied to telecommunications is due to G. F. ROSS in 1973 [1]. From a theoretical point of view major breakthroughs were achieved during the last decade. Among all the various transmission techniques using UWB labelled modulations, the efficiency of *Impulse Radio* (IR) was pointed out. Two categories of receiver strategy were then envisioned: on the one hand optimal coherent rake receivers involving perfect channel knowledge on resolved paths, see M. Z. WIN & R. A. SCHOLTZ [2], on the other sub-optimal incoherent receivers essentially involving energy detection and therefore relaxed channel estimation, see S. VERDÚ [3] and Y. SOUILMI & R. KNOPP [4].

With respect to the numerous number of significative paths [5] and signal distortion produced by both antennas and material propagation [6], synchronization and generally speaking channel estimation in IR schemes turns out to be a critical point to design rake receivers; especially for applications including severe mobility. As we here deliberately stress low-cost hardware architectures, asynchronous methods are favoured, since they require relaxed synchronization constraints. Pursuing the initial work of S. VERDU and R. KNOPP, where essentially prior channel statistics are available to the receiver, our approach includes as a new deterministic parameter an estimation of available energy. Moreover a relevant paper by P. A. HUMBLET [7] addresses a similar formal problem, but dedicated to optical photodetection.

The following development starts with an insight into the choice of an *On-Off Keying* (OOK) modulation generalized over multiple sub-bands and a channel propagation model description. Afterward the optimal demodulation problem on a particular sub-band is set. As mentioned above its specificity consists in using a prior information made of the approximative channel delay spread and the available energy level. Deriving statistical considerations, one shows the demodulation stage consists in a non-trivial energy threshold comparison, for which a simple and original analytical expansion can be given, making the implementation cost-effective. In order to illustrate the potential of these principles numerical applications based on IEEE 802.15.3a are then detailed. Possible transceiver implementations involving mainly analog devices conclude the argumentation.

II. CONTEXT SETTING

A. On-Off Keying justification

Let's start with a brief argumentation on the choice of an OOK modulation.

As a good understanding of the propagation aspects for UWB is mandatory, let's examine typical characteristics of a UWB channel (see FIG.1). As shown by propagation measurements [5], typical values of delay spread T_d are

30 to 150 ns for distances varying from 1 to 10 meters while the number of significant paths can be up to 60 to recover 85% of available energy.

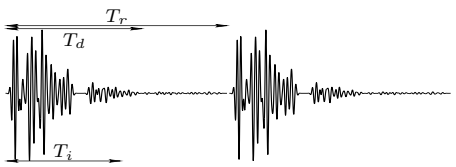

Fig. 1. Repetition time, delay spread and integration time.

In order to achieve high data rates at low-cost, it seems reasonable to prohibit complex equalization processes, in that context avoiding inter-symbol interference is a natural idea. Thus, the symbol repetition period T_r is chosen such as $T_r \geq T_s + T_d$, where T_s is the duration allocated to the symbol waveform. For high data rates IR schemes, we aim at carrying elementary symbol information within a single pulse duration $T_s \approx T_{\text{pulse}} \ll T_d$ (a typical pulse bandwidth is roughly a few GHz). As a consequence, we can simply impose $T_r \geq T_d$.

Favoring non-coherent demodulation, and thus a receiver working as an energy detector, information is preferably carried by signal amplitude rather than its phase. It naturally leads us to consider Pulse Amplitude Modulation. In that case an OOK modulation appears to be a suitable candidate since it possesses a good optimality considering a non-coherent demodulation (see Verdú and flash-signaling [3]). Ultimately and so as to increase the system capacity while preserving these properties, we propose to duplicate this basic scheme on several separate sub-bands (in practice from 8 to 24).

The adopted non-coherent receiver structure per sub-band is then the following:

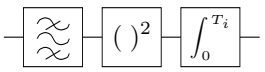

Fig. 2. Non-coherent receiver: energy integration.

where T_i denotes the energy integration time devoted to a symbol demodulation. Though an optimization should be investigated, for our numerical applications T_i and T_r will be roughly chosen as the channel delay spread T_d.

B. Channel model

Comparison between system performances involves a common channel model. In the sequel, for an emitted pulse with waveform $p(t)$, the received signal will be:

$$y(t) = \sum_k A_k p(t - \tau_k) + w(t)$$

where k indexes the paths of the channel. The τ_k denote the path delays and are monotonically increasing with k while the A_k denote their amplitude. Whereas in III we consider a realization of a particular radio link, *i.e* parameters A_k, τ_k are fixed, for the system performances shown in IV a statistical behavior is required. We will use the four channel models of IEEE 802.15.3a [5], which corresponds to indoor configurations within a range of a few meters. The additive term $w(t)$ denotes the thermal noise whose two-sided spectral density is $N/2$.

Note that a model including a waveforms $\tilde{p}_k(t)$ instead of the fixed waveform $p(t)$, emphasizing the distortions undergone by propagation, would not impact the following development, provided the spectral support of $p(t)$ is not significantly affected by channel effects.

III. Analysis

We shall consider a modulation scheme in accordance with the description II.A. The system is assumed to include a preamble step with the purpose of performing a coarse synchronization. This phase enables to estimate the duration T_d encompassing the most significant paths. The symbol repetition period $T_r \geq T_d$ is derived as well as the integration duration $T_i \leq T_d$ (see FIG.1 and 2). Concentrating on a particular sub-band of width B in which a pulse of general waveform $p(t)$ is located (see [2] for waveform examples) , the transmitted signal is then:

$$s(t) = \sum_{n=-\infty}^{+\infty} \eta_n \, p(t - nT_r)$$

where $\eta_n \in \{0, 1\}$ are the emitted bit in the OOK scheme.

A. Decision problem setting

From the receiver point of view, the demodulation stage exacts to face the two following hypotheses:

$$\begin{cases} H_0: \quad x = \displaystyle\int_0^{T_i} [n(t)]^2 \, dt & \text{(bit 0)} \\ H_1: \quad x = \displaystyle\int_0^{T_i} [s_{\text{rec}}(t) + n(t)]^2 \, dt & \text{(bit 1)} \end{cases}$$

where, with respect to the model depicted in II.B, $s_{\text{rec}}(t)$ is the deterministic part of $y(t)$ while $n(t)$ corresponds to the noise $w(t)$, each of them filtered in the appropriate sub-band.

With respect to the integrator output x, the demodulation stage consists in deciding "at best" between H_0 and H_1, *i.e* intending to minimize the error probability.

As a major improvement on usual non-coherent approaches, besides the noise spectral density $N/2$, B and T_i, the estimation of the signal energy $E = \int_0^{T_i} s_{\text{rec}}^2(t)dt$ (deterministic for the fixed channel parameters: A_k, τ_k) will enrich the *a priori* channel knowledge. This estimation could be naturally performed during the preamble step thanks to appropriate unbiased estimators (see [7] for statistics of x under $(H_i)_{i\in 0,1}$).

B. Optimal threshold

Appropriate statistical methods based on the likelihood ratio test (see VAN TREES [8]) show the optimal decision rule consists in comparing the statistic x to a predefined threshold ρ_{opt} and deciding according to:

$$x \underset{H_0}{\overset{H_1}{\gtrless}} \rho_{\text{opt}}$$

where ρ_{opt} is the solution of $p_0(x) = p_1(x)$ assuming equal likely bits 0 and 1 , the $p_i(x)$ being the probability density function (*pdf*) under the hypothesis $(H_i)_{i\in\{0,1\}}$.

These are shown to be central (resp. non-central) Chi-square distribution (χ^2) for H_0 (resp. H_1) (see [7] [8]):

$$\begin{cases} p_0(x) = \dfrac{1}{N\Gamma(M)} \left(\dfrac{x}{N}\right)^{M-1} \exp\left(-\dfrac{x}{N}\right) \\ p_1(x) = \dfrac{1}{N} \left(\dfrac{x}{E}\right)^{\frac{M-1}{2}} \exp\left(-\dfrac{x+E}{N}\right) I_{M-1}\left(2\dfrac{\sqrt{xE}}{N}\right) \end{cases}$$

where $2M = 2BT_i + 1$, Γ denotes the EULER function and I_n the n^{th} BESSEL function of the first kind.

These *pdf* can be expressed as functions of the normalized variable $x/N \geq 0$ and the number of fixed parameters involved is advantageously reduced to two quantities. These are the energy ratio $L = E/N$ and M where $2M = 2BT_i + 1$ is the dimension of the space of functions whose energies are concentrated in a bandwidth B and time T_i, which is the number of degrees of freedom of the χ^2 distributions as well.

In practice, the computation of ρ_{opt} has to be performed efficiently. It is the reason why we now aim at expanding ρ_{opt}/N into an operative formula depending on L and M. We propose the following method.

Let's start with the asymptotic equivalent for a fixed M:

$$I_{M-1}(u) \sim K u^{-\frac{1}{2}} \exp u$$

for a positive K and $u \to +\infty$, reporting in $p_0(\rho_{\text{opt}}) = p_1(\rho_{\text{opt}})$, $\overline{\rho} = \rho_{\text{opt}}/N$ (function of L) must satisfy:

$$(L\overline{\rho})^{\frac{M}{2}-\frac{1}{4}} \exp L \sim K\Gamma(M) \exp(2\sqrt{L\overline{\rho}})$$

for $\overline{\rho}L \to +\infty$. Taking the logarithm:

$$2 - \sqrt{\frac{L}{\overline{\rho}}} - \left(\frac{M}{2} - \frac{1}{4}\right) \frac{\ln \overline{\rho}L}{\sqrt{\overline{\rho}L}} \to 0$$

Thus $\sqrt{\frac{L}{\overline{\rho}}} \to 2$ and $\overline{\rho} \sim L/4$ for $\overline{\rho}L \to +\infty$. Equivalently $\overline{\rho} \sim L/4$ for $L \to +\infty$.

Then processing numerically $\rho_{\text{opt}}/N - L/4$, we propose an interpolation yielding the original expression:

$$\frac{\rho_{\text{opt}}}{N} = \frac{L}{4} + M + \sqrt{M-1}\,\phi(L)$$

where ϕ is a tabulated function depending on the variable L alone (see FIG. 3). An *a posteriori* verification validates this approximation with $\pm 1\%$ error.

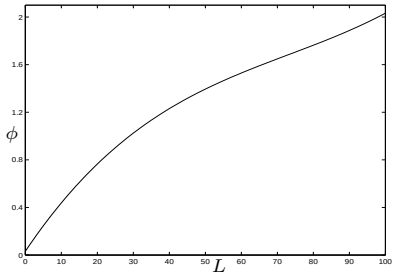

Fig. 3. Plot of the ϕ function.

Remark: in case of a non-ideal filter, these calculations can also be carried out, taking into account the exact filter response $h(t)$ (see MIDDLETON [9]).

C. Error probability

Let's denote $\rho = \rho_{\text{opt}}$ the optimal threshold. As shown in [7], the probability of deciding H_1 whereas no signal had been sent is given by:

$$P(1|0) = e^{-\rho/N} \sum_{k=1}^{\lfloor M \rfloor} \frac{(\rho/N)^{M-k}}{\Gamma(M-k+1)}$$

where $\lfloor M \rfloor$ denotes the integer part of M. Conversely, the probability of deciding H_0 whereas bit 1 was sent is:

$$P(0|1) = 1 - Q_M\left(\sqrt{2L}, \sqrt{2\frac{\rho}{N}}\right)$$

where Q is the generalized Marcum function:

$$Q_m(a,b) = \frac{1}{a^{m-1}} \int_b^\infty x^m e^{-\frac{x^2+a^2}{2}} I_{m-1}(ax)dx$$

In the expression of $P(0|1)$, L is equal to E/N with E the energy of the received pulse (when a bit 1 has been sent). Then, the error probability expressed as a function of the mean received energy $\mathcal{E} = E/2$ is the following analytical formula:

$$P_e = \frac{1}{2} - \frac{1}{2} Q_M\left(\sqrt{\frac{4\mathcal{E}}{N}}, \sqrt{\frac{2\rho}{N}}\right) + \frac{e^{-\frac{\rho}{N}}}{2} \sum_{k=1}^{\lfloor M \rfloor} \frac{(\rho/N)^{M-k}}{\Gamma(M-k+1)}$$

D. Curves and comments

On FIG. 4 are plotted performances P_e versus $\mathcal{E}/N$ for various receivers, where $\mathcal{E}$ is the deterministic amount of energy eventually processed. It shows that to achieve comparable P_e the non-coherent OOK receiver has to increase its link budget by 4 to 5 dB with respect to a coherent BPSK receiver, for typical values of $M \approx BT_i$ (between 7 and 25, see IV.B.).

But, for a fair comparison, we have to keep in mind that whereas the proposed non-coherent receiver is able to integrate almost the whole available energy, a coherent rake receiver has a limited number of fingers and will recover a small part of it. Thus, to be competitive, the latter should recover at least from 33% to 40% of the whole energy (4 to 5 dB difference). Taking up such a challenge is quite unlikely due to the propagation characteristics pictured in II.A.; this obviously confers an inherent advantage to the non-coherent scheme.

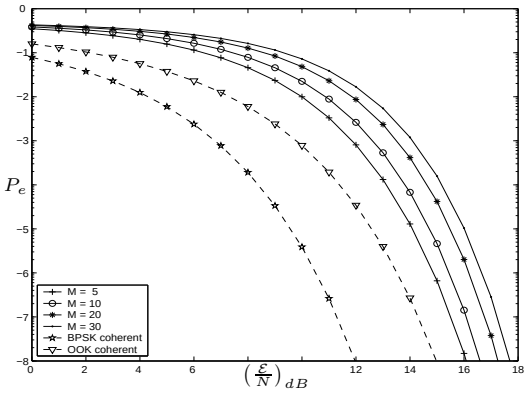

Fig. 4. Error probability versus $\mathcal{E}/N$ for different values of M.

IV. System performances

A link budget determination for typical environments according to IEEE 802.15.3a channel models will now give realistic achievable data rates.

A. Link budget methodology

The required parameters are detailed in the table I.

Transmitter: E_{TX} is the maximum mean transmitted energy allowed by regulation (FCC, [10]) according to the band B and the repetition period T_r.

Channel: The signal undergoes an attenuation denoted $L_{tot} = L_1 + L_2 - L_3$. The attenuation L_1 at 1 meter results from the propagation through antennas. L_2 relates to the free space propagation without multipath. L_3 is the gain brought by the multipath energy integration.

For a good understanding of L_3, let's notice that if the energy is integrated over the single direct path alone, then $L_3 = 0$ dB. Of course, due to the diversity provided by the UWB channels, an important gain is brought by multipath integration over the duration T_i. This gain is computed according to the IEEE 802.15.3a channel models [5], for a given bandwidth B and for different types of channel models (CM). The types 2, 3 and 4 are all NLOS (Non Line Of Sight) and respectively valid from 0 to 4 meters, from 4 to 10 meters and for extreme multipath configurations.

Receiver: The received energy E can be derived from E_{TX} and L_{tot}. Finally, from the above theoretical study, P_e is easily obtained for the given link budget.

Transmitter		
Band	B	MHz
Repetition period	T_r	ns
Energy at TX	$E_{TX} = f(B, T_r)$	dBJ
Data per band	$R = 1/T_r$	Mbit/s
Channel		
Distance	d	m
Path loss at 1 meter	$L_1 = 20\log_{10}(4\pi f_c/c)$	dB
Path loss at d meters	$L_2 = 20\log_{10}(d)$	dB
Multipath integration gain	L_3	dB
Channel loss	L_{tot}	dB
Receiver		
Energy at RX	$E_{RX} = E_{TX} - L_{tot}$	dBJ
Noise density	$N_0 = -204 \equiv -174$dBm/Hz	dBJ
RX noise figure	$N_f = 11$	dB
Energy to noise ratio	$(E/N)_{\text{dB}} = E_{RX} - N_0 - N_f$	dB
Degrees of freedom	$2M = 2BT_i + 1$	
Error probability	$Pe = f(E/N, M, \rho)$	

TABLE I. Link budget analysis table.

B. Results

In the table II, numerical results of three link budget samples are presented.

Bit rate	**150**	**240**	**600**	Mbit/s
d	**10**	**5**	**3**	m
B	500	500	250	MHz
N_{band}	12	12	24	
T_r	80	50	40	ns
CM	4	3	2	
T_i	50	40	30	ns
$\overline{P}_e$	10^{-5}	10^{-5}	10^{-5}	

TABLE II. Performances samples.

As required for a IEEE 802.15.3a proposal, 100 channels (different sets of A_k, τ_k) are computed according to the statistical model [5], each of them giving an available energy $E = 2\mathcal{E}$ at the receiver input as explain above. Then, the mean of the error probability ($\overline{P}_e$) is taken over the 90 most favorable $\mathcal{E}$.

V. Hardware implementation

A. General considerations

The hardware implementation greatly benefits from the relaxed constraint offered by the asynchronous approach.

Primarily, only a coarse synchronization is needed (an error of 2 ns $\ll T_d \approx 50$ ns is acceptable), which makes the system robust against the clock jitter and every triggering inaccuracy. Secondly, since the treatment is based on energy, the transceiver performances are nearly insensitive to distortion and phase non-linearity of devices like

antennas, amplifiers or filters. Finally, a low power consumption is achieved thanks to the use of mainly analog and passive devices.

B. Implementation sketches

The transmitter architecture depicted on FIG. 5 uses a filter bank of up to 24 adjacent filters. At the input of this filter bank, a UWB pulse (covering the whole $3-10$ GHz bandwidth) is generated with a repetition period T_r. On each line, the relatively narrow-band (from 250 to 500 MHz) pulses are modulated by an OOK modulation at the rate of $1/T_r$.

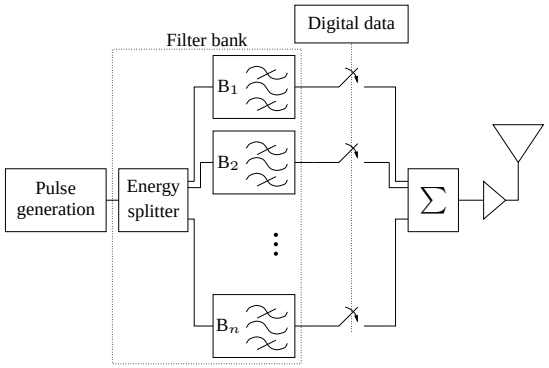

Fig. 5. Transmitter implementation sketch 1.

Conversely, a second solution uses a bank of local oscillators ensuring the frequency transposition toward each sub-band. Notice that oscillators are only used to provide transposition, coherence is not required. The OOK modulation controls the own activation of each oscillator. In this solution the constraint on the pulse width to generate is relaxed (2 ns for 500 MHz bandwidth). In both sketches, every "narrow-band" pulses are added producing a UWB signal which is sent through the antenna. An interesting feature to notice is that an easy power control in each sub-band is possible. This kind of flexibility can be useful to fulfill a regional PSD mask.

On the receiver side (FIG. 6), a filter bank splits the signal on the same sub-bands as the transmitter. Then on each parallelized stage, a square law device and an integrator follow, the output of which is sampled at a rate of $1/T_r$ before demodulation.

CONCLUSION

This paper presents a simple non-coherent architecture providing high data rate with impulse radio. The encouraging performances obtained show the obvious potential of these principles and the mainly analog-oriented transceiver architecture could be fruitfully capitalized for low-cost applications.

In order to go closer into related matters, we could point out the following key points.

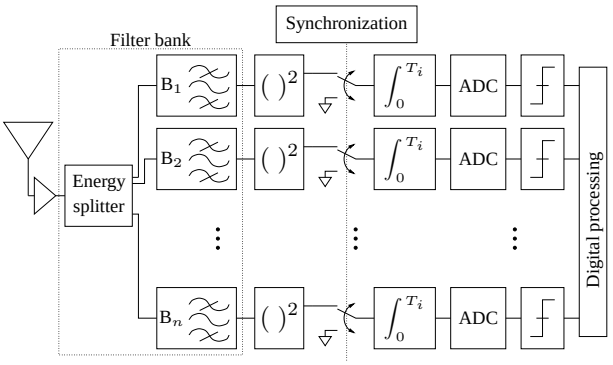

Fig. 6. Receiver implementation sketch.

Further studies on inter-band interferences based on precise passband filter characteristics are to be carried out to complete the system dimensioning.

Relaxed synchronization methods based on asynchronous time-hopped signal detection have also been investigated to enable fast channel delay spread estimation. However space limitation prevents us from developing these topics in this paper.

From a system point of view, usual *Medium Access Control* (MAC) may be re-visited taking benefit from energy detection techniques while piconet division may favour the inherent frequency separation properties in such a system.

ACKNOWLEDGMENT

We wish to thank CLAIRE MEUNIER who closely participated to our mathematical developments and GWILLERM FROC whose experience as a physicist encouraged us to investigate these principles.

REFERENCES

[1] Ross, G. F.; "Transmission and reception system for generating and receiving baseband duration pulse signals for short baseband pulse communication system," *U.S. Patent 3.728.025,* July 31, 1973.

[2] Win, M.Z.; Scholtz, R.A.; "Impulse radio: how it works," *IEEE Communications Letters,* Vol. 2, No. 2, Feb. 1998, pp. 36-38.

[3] Verdú, S.; "Spectral efficiency in the wideband regime," *IEEE Transactions on Information Theory,* Vol. 48, No. 6, June 2002, pp. 1319-1343.

[4] Souilmi, Y.; Knopp, R.; "Challenges in UWB signaling for adhoc networking," *DIMACS Workshop on Signal Processing for Wireless Transmission,* Oct. 2002

[5] IEEE; "Channel modeling sub-committe report," *IEEE P802.15 Wireless Personal Area Networks,* Feb. 7, 2003.

[6] Tchoffo Talom, F.; Uguen, B; Plouhinec, G. Chassay and F. Sagnard, "Study of interactions effects on Ultra WideBand signals propagation," *Proc. IEEE IWUWBS 2003 Conf.,* June 2003.

[7] Humblet, P. A.; Azizoglu, M.; "On the bit-error rate of lightwave systems with optical amplifiers," *Journal of Lightwave Technology,* vol. 9, pp. 1576-1582, Nov. 1991.

[8] Van Trees, H. L.; "Detection, estimation and modulation theory, part I," *Wiley, New York,* 1968.

[9] Middleton, D.; "An introduction to statistical communication theory," *McGraw-Hill, New York,* 1960

[10] Federal Communications Commission "First report and order," *ET Docket No. 98-153,* April 22, 2002.